


RESEARCH ARTICLE

Open Access



# Atmospheric resuspension of insoluble radioactive cesium-bearing particles found in the difficult-to-return area in Fukushima

Peng Tang<sup>1</sup> , Kazuyuki Kita<sup>1\*</sup>, Yasuhito Igarashi<sup>1,2\*</sup>, Yukihiro Satou<sup>3</sup>, Koutarou Hatanaka<sup>1</sup>, Kouji Adachi<sup>4</sup>, Takeshi Kinase<sup>5</sup>, Kazuhiko Ninomiya<sup>6</sup> and Atsushi Shinohara<sup>6</sup>

## Abstract

The deposition of insoluble radiocesium-bearing microparticles (CsMPs), which were released from the Fukushima Daiichi Nuclear Power Plant (F1NPP) accident in March 2011, has resulted in the widespread contamination of eastern Japan. Obviously, these deposited insoluble CsMPs may become the secondary contamination sources by atmospheric migration or other environmental transferring process; however, the understanding of the transport mechanism remains non-elucidation, and the relevant evidence has not been directly provided. This study, for the first time, provides the direct evidence for the resuspension of these insoluble CsMPs to the atmosphere from (1) proximity of <sup>137</sup>Cs radioactivity and resemblance of the morphology and the elemental compositions of CsMPs in the samples of soil and aerosol derived from the same sampling site, (2) the special characteristics of the resuspended CsMPs of which the ratios of Na/Si, K/Si and/or Cs/Si were smaller than those from the initially released CsMPs collected at either long distance or near F1NPP, which can be ascribed to the slowly natural corrosion of CsMPs by the loss of the small amount of soluble contents in CsMPs, and (3) high CsMPs concentration of 10 granules/g in the surface soil of our sampling site and high resuspension frequency of CsMPs in spring when predominant suspended particles were soil dust. Specifically, 15 single CsMPs were successfully isolated from the aerosol filters collected by unmanned high-volume air samplers at a severely polluted area in Fukushima Prefecture, about 25 km away from F1NPP, from January 2015 to September 2019. The mean diameter of these CsMPs was  $1.8 \pm 0.5 \mu\text{m}$ , and the average <sup>137</sup>Cs radioactivity was  $0.35 \pm 0.23 \text{ Bq/granule}$ . The contribution rate of the resuspended CsMPs to the atmospheric radiocesium was estimated from the ratio of <sup>137</sup>Cs radioactivity of a single CsMP to that of the aerosol filter to be of  $23.9 \pm 15.3\%$ . There has been no considerable decreasing trend in the annual CsMP resuspension frequency.

**Keywords:** Resuspension, Radiocesium, Water-insoluble radiocesium-bearing microparticles (CsMPs), Fukushima accident, Aerosol

## Highlights

1. This study, for the first time, provides the direct evidence of natural resuspension contribution of the insoluble radiocesium-bearing microparticles (CsMPs) to the atmospheric radiocesium.

\*Correspondence: kazuyuki.kita.iu@vc.ibaraki.ac.jp; igarashi.yasuhito.4e@kyoto-u.ac.jp

<sup>1</sup> Graduate School of Science and Engineering, Ibaraki University, 2-1-1 Bunkyo, Mito, Ibaraki 310-8512, Japan

Full list of author information is available at the end of the article

2. This study introduces the evaluating method of resuspension contribution rate of CsMPs by the ratio of the radioactivity of  $^{137}\text{Cs}$  in a single CsMP to that of aerosol filter.
3. This work reveals that there is no clear downward trend in the annual frequency of CsMP resuspension and a slightly higher frequency in the springtime is attributed to high wind gust speed and low moisture of topsoil, though the distribution of CsMP resuspension is observed in each season.

## 1 Introduction

### 1.1 Accident

The Fukushima Daiichi Nuclear Power Plant (F1NPP) accident was triggered by the 9.0-magnitude Tohoku-Oki earthquake and the subsequent tsunami on March 11, 2011 (Committee and on the Accident at the Fukushima Nuclear Power Station of Tokyo Electric Power Company 2011; Fuchigami and Kasahara 2011), which resulted in the complete loss of all power and over-heat and over-pressurization of Units 1–3 (there are 6 Units in F1NPP and Units 4–6 had been “shut down” for regular maintenance prior to the earthquake (Tokyo Electric Power Company Holdings 2011)). Over the subsequent several days, despite the attempt to inject cooling water and/or perform venting operations for Units 1–3 (starting at 10:40 JST on March 12 (Fuchigami and Kasahara 2011), 10:15 JST on March 13 (Tokyo Electric Power Company Holdings 2011) and 08:41 JST on March 12 (Hatamura et al. 2014), respectively), hydrogen explosions could not be avoided at Units 1 and 3 (at 15:36 JST on March 12 and 11:01 JST on March 14 (Committee and on the Accident at the Fukushima Nuclear Power Station of Tokyo Electric Power Company 2011)). Thus, a large quantity of radioactive materials was released into the atmosphere (Igarashi et al. 2015), the land (Yoshida and Kanda 2012; Yoshida and Takahashi 2012), and the Pacific Ocean (Hirose 2016). Specifically, the amount of total atmospheric release of  $^{137}\text{Cs}$  was up to 15–21 PBq (1 PBq =  $10^{15}$  Bq), and 3–6 PBq was directly deposited onto the land (Aoyama et al. 2020). The rest of the  $^{137}\text{Cs}$  was distributed over the North Pacific, which was quantified to be 15–18 PBq (Aoyama et al. 2020). Moreover, Steinhäuser et al. (Steinhäuser et al. 2014) reported that the highly contaminated area, with  $^{137}\text{Cs}$  levels exceeding  $185 \text{ kBq m}^{-2}$ , spread approximately  $1700 \text{ km}^2$  in Fukushima Prefecture.

### 1.2 Radiocesium-bearing microparticles

Water-insoluble radiocesium-bearing microparticles (hereafter CsMPs) (Adachi et al. 2013; Igarashi et al. 2019a) were released and deposited in the environment

by the F1NPP accident. In recent several years, research on the morphology, elemental compositions, classifications, and emission sources of CsMPs has been comprehensively reported (Adachi et al. 2013; Igarashi et al. 2019a; Satou et al. 2018; Snow et al. 2016). Specifically, Adachi et al. (2013) first reported that spherical CsMPs mainly contained O, Fe, and Zn as well as other trace elements. These CsMPs were referred to as the released and deposited CsMPs in early stage of the F1NPP accident (Ishizuka et al. 2017). Based on the difference of size and structure as well as the difference in the isotopic ratio of  $^{134}\text{Cs}/^{137}\text{Cs}$ , the CsMPs have been classified into type A (possibly derived from Unit 2 or 3 with a size of less than  $10 \mu\text{m}$  and  $^{134}\text{Cs}/^{137}\text{Cs} \approx 1.0$ ) and type B (perhaps released from Unit 1 with a size of more than  $100 \mu\text{m}$  and  $^{134}\text{Cs}/^{137}\text{Cs} \approx 0.9$ ) (Igarashi et al. 2019a; Satou et al. 2018). There are also reports suggesting that type A CsMPs were derived from Unit 2 (Hidaka 2019) or Unit 1 (Abe et al. 2014). Moreover, the glassy state of CsMPs implied water insolubility [discussed in detail in references (Adachi et al. 2013; Niimura et al. 2015)] and comparatively persistent toxicity and hazards in the terrestrial environment (Suzuki et al. 2020) ( $^{137}\text{Cs}$  has a half-life of 30.2 years (Press 2015)). The high-dose internal radiation exposure by the inhalation of radioactive aerosols and the consumption of food associated with radioactive material is the most concerning health hazard (Yamamoto et al. 2019; Shannon 2012; Nakamura 2020). In order to assess and reduce the risk of radiocesium inhalation (Higaki et al. 2020) and the intake of food (Miura et al. 2021; Nihei et al. 2018) contaminated by CsMPs, it is necessary to understand its distribution and transport in the secondary processes in the environment.

### 1.3 Resuspension of radiocesium

Hirose (2013) found that the deposition of the early-stage released radiocesium was significant from March to June 2011 and that an obvious decrease in radiocesium deposition rate occurred after July 2011. Hirose (2020) concluded that most of the F1NPP-derived  $^{137}\text{Cs}$  deposited on the ground surface remained in the surface soil layer as a potential secondary source of atmospheric  $^{137}\text{Cs}$ , and Tanaka et al. (2012) reported that more than 90% of the radiocesium was fixed within the top 5 cm of the profile. Although the F1NPP accident has passed for about 10 years, most of the  $^{137}\text{Cs}$  is thought to remain there (Matsuda et al. 2015), and thus the decontamination by removal of topsoil was conducted in Fukushima Prefecture (Mishra et al. 2015; Evrard et al. 2019). Resuspension of radiocesium refers to the secondary migration of the deposited radiocesium into the atmosphere from surfaces and terrestrial ecosystems by winds (Ochiai et al. 2016), biomass burning (Igarashi et al. 2015), and other

different anthropogenic disturbances (Yamaguchi et al. 2012; Akimoto 2015), which can be found in the reports about the F1NPP accident (Ochiai et al. 2016; Yamaguchi et al. 2012; Akimoto 2015; Kinase et al. 2018) and the Chernobyl Nuclear Power Plant accident (Wagenfeil and Tschiersch 2001; Garger et al. 1996; Yoschenko et al. 2006). Regarding the issue, Igarashi et al. (2015) emphasized, through their observation and data analysis of radiocesium in air over Tsukuba and Ibaraki, that “elucidating the secondary emission processes of the F1NPP radionuclides remains an imminent scientific challenge, especially for heavily polluted areas. Secondary sources can include soil dust suspension from polluted earth surfaces, emissions from polluted vegetation and forests, and volatilization and release from combustion of polluted garbage and open field burning. Although the main emission sources are not yet well understood, this elucidation must be performed as soon as possible.” Significantly, this process is an uncontrollable route that can cause widespread secondary contamination (Nihei et al. 2018) in previous noncontaminated or decontaminated areas. Although the radioactivity level of resuspension (Igarashi et al. 2015; Kinase et al. 2018) was a few orders of magnitude lower than that of the early-stage released, it would be a matter of public concern, especially for the evacuated people who lived in difficult-to-return areas.

Hirose (2013) suggested that the second increase in atmospheric radiocesium in the spring 2012 can be attributed to the resuspension process. Moreover, seasonal variations of radiocesium in aerosol samples were observed in severely contaminated areas of Fukushima Prefecture (Ishizuka et al. 2017; Kinase et al. 2018; Kita et al. 2018; Igarashi et al. 2019b), being explained as the result of radiocesium resuspension because the observed seasonal dependence of the atmospheric radiocesium concentration cannot be interpreted from direct or delayed primary release from F1NPP accident site (Igarashi et al. 2019b). Specifically, Ishizuka et al. (2017) measured and modeled the particle size distribution of suspended soil dust carrying radiocesium considering different soil textures. Kinase et al. (2018) and Igarashi et al. (Igarashi et al. 2019b) discussed possible resuspension-hosting sources and showed that soil particles (Kaneyasu et al. 2012) can be significant in the spring-time and that bioaerosols such as pollens (Nakagawa et al. 2018), spores (Igarashi et al. 2019b), and microorganisms (Kinase et al. 2018) can be a major host particle in summer and autumn. Kajino et al. (2016) modeled the resuspension of  $^{137}\text{Cs}$  from bare soil and forest ecosystems and suggested a similar seasonal change of the resuspension host particle to above-mentioned studies, namely, the high radiocesium concentration can be observed in warm seasons and the low can be obtained

in cold seasons. They also estimated respective resuspension rates of  $1\text{--}2 \times 10^{-6} \text{ day}^{-1}$  (Kajino et al. 2016). These results were helpful to estimate the inhalation dose (EPA 1977; Garger and Talerko 2020). However, research on the resuspension of radiocesium has still been insufficient, and both observational and theoretical model studies are necessary for a quantitative understanding. Notably, these studies did not discuss the resuspension of the CsMPs.

Higaki et al. (2014) reported that the main sources of radiocesium adhered to non-woven fabric face masks, which were worn both outdoors and indoors by 68 residents living in eastern Japan in the spring of 2012, were fugitive dust and CsMPs (Higaki et al. 2020) (the masks were worn by the Fukushima residents in the spring of 2013). The CsMPs were also isolated from Japanese spinach (Nihei et al. 2018). Although these results suggested the possibilities of the resuspension of CsMPs from the ground to the atmosphere, there has been no evidence to indicate that it occurred naturally (without anthropogenic interferences) and no discussion about the special features of the collected CsMPs to demonstrate whether they are derived from resuspension or other reasons. This study, for the first time, provides the direct evidence of resuspension of the CsMPs in the monitoring duration at our sampling site, and explains the transport variables and mechanism of the CsMPs. Therefore, this study aims at (1) detection and isolation of highly radioactive granules from aerosol and soil samples collected at a severely polluted area to identify them as CsMPs by analyses of their morphology and elemental compositions, (2) describing the possibility of the natural resuspension of CsMPs to the atmosphere and (3) evaluating the frequency of CsMP resuspension and its contribution ratio to the whole atmospheric concentration of radiocesium.

## 2 Experiments and methods

### 2.1 Sample collection

#### 2.1.1 Sampling of aerosols

Aerosol samples were collected at a site ( $37.6^\circ \text{ N}$ ,  $140.8^\circ \text{ E}$ , and altitude 438 m) located in a highly contaminated zone that was difficult for residents to return to (approximately 25 km northwest from the F1NPP), as shown in Fig. 1. Details of the sampling site are described elsewhere (Ishizuka et al. 2017; Kinase et al. 2018; Igarashi et al. 2019b; Kajino et al. 2016). Aerosol samples were collected on quartz-fiber filters (2500QAT-UP, Pall Corp., NY, USA or QR100, Advantech, Tokyo, Japan) with high-volume samplers (HV samplers; HV-1000R/E, Sibata Scientific Technology, Ltd., Saitama, Japan and 120SL, Kimoto Electric Co. Ltd., Tennoji, Osaka, Japan) at a sampling air flow rate of  $0.7 \text{ m}^3 \text{ min}^{-1}$  from January 2015 to September 2019.

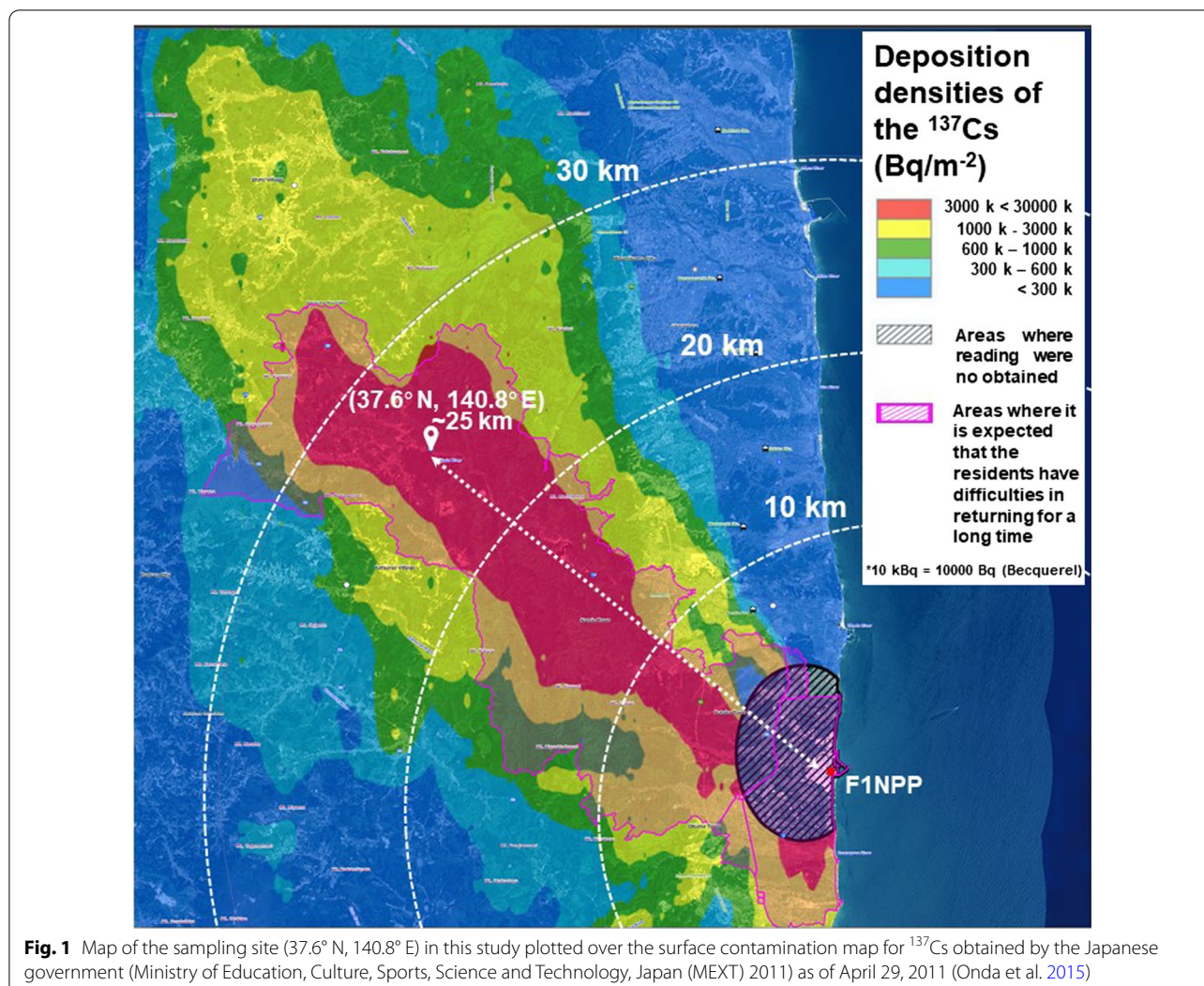


**Fig. 1** Map of the sampling site ( $37.6^\circ\text{ N}$ ,  $140.8^\circ\text{ E}$ ) in this study plotted over the surface contamination map for  $^{137}\text{Cs}$  obtained by the Japanese government (Ministry of Education, Culture, Sports, Science and Technology, Japan (MEXT) 2011) as of April 29, 2011 (Onda et al. 2015)

We used the aerosol samples collected in 2015, 2016, 2018, and 2019 because the aerosol sampling was interrupted for several months in 2017. Additionally, aerosol samples with different aerodynamic diameters were also collected separately on slotted quartz-fiber filters using an HV sampler with a seven-stage cascade impactor (TE-230, Tisch Environmental Inc., OH, USA) with slotted quartz-fiber filters. The aerodynamic size-distribution ranges with a collection efficiency exceeding 50% were sampled as follows: Q1 ( $>10.3\ \mu\text{m}$ ), Q2 ( $4.2\text{--}10.3\ \mu\text{m}$ ), Q3 ( $2.1\text{--}4.2\ \mu\text{m}$ ), Q4 ( $1.3\text{--}2.1\ \mu\text{m}$ ), Q5 ( $0.69\text{--}1.3\ \mu\text{m}$ ), Q6 ( $0.39\text{--}0.69\ \mu\text{m}$ ), and Q7 ( $<0.39\ \mu\text{m}$ , working as a backup filter) at a sampling air flow rate of  $0.556\ \text{m}^3/\text{min}$ . Note that the aerosol samples were successively taken by 10 timer-controlled HV samplers without anthropogenic interference, except for replacing the sampling filters over the course of a few hours every 2–4 weeks. In all sampling processes, aerosol

filter samples were collected at a height of 1.2 m above the ground. The sampling periods ranged from 3 days to 4 weeks.

### 2.1.2 Collection of soil samples

About 200 g of surface soil samples was collected on June 25, 2016, at the same site as the aerosol-sampling location with a  $10 \times 10\ \text{cm}^2$  area and 1.5 cm depth and were transported to the laboratory and stored at ambient temperature. They were homogenized in a plastic bag (Onda et al. 2015) for measurement of their radioactivity and stored for further analysis. For extracting the CsMPs, approximately 2.5 g soil sample was randomly retrieved (the radioactivity was  $173.6 \pm 2.00\ \text{Bq/g}$  and  $166.2 \pm 0.40\ \text{Bq/g}$  for  $^{134}\text{Cs}$  and  $^{137}\text{Cs}$ , respectively). The radioactivity data in this study were all corrected back to March 11, 2011, 14:46 JST.

## 2.2 Detection and isolation of highly radioactive granules

An imaging plate (IP) system (CR×25P portable computed radiography, GE Measurement & Control, Massachusetts, USA) and a micromanipulator (Axis Pro; Micro Support Corp., Shizuoka, Japan) were used to detect and isolate CsMPs from the aerosol filters. The isolation procedure of CsMPs from the aerosol filters and from the soil samples was conducted as the similar dry process (without use of water) of Adachi et al. (2013) and Satou et al. (2016), respectively.

## 2.3 Measurement of gamma-ray spectrometry and SEM observation

The gamma-ray peak intensities at 605 and 662 keV were used to identify and determine the radioactivities of  $^{134}\text{Cs}$  and  $^{137}\text{Cs}$ , respectively (Satou et al. 2016). Identification of the CsMPs was based on the morphology and elemental compositions of the single highly radioactive particle. The observation of the morphology and elemental compositions was conducted with an SEM (SU3500, Hitachi High-Technologies Co., Tokyo, Japan) equipped with energy-dispersive X-ray spectroscopy (EDS: X-max 50 mm, Horiba Ltd., Kyoto, Japan) for aerosol CsMPs and a field emission SEM (JSM-7800F, JEOL Ltd. Tokyo, Japan) for visualizing soil CsMPs and water-immersed aerosol CsMPs.

## 3 Results and discussion

### 3.1 Identification of resuspension of CsMPs

#### 3.1.1 Aerosol CsMPs (A-CsMPs)

Twenty highly radioactive granules were detected from the aerosol samples by using IP imaging, 15 of which have been successfully isolated, and the rest of which was lost during the isolation procedures. Their SEM observation images are shown in Fig. 2, and the detailed information regarding radioactivity and elemental compositions is given in Table 1 and Additional file 1: Table S1. These results indicate that all isolated granules have characteristics corresponding to those reported for type A CsMPs (Igarashi et al. 2019a; Satou et al. 2018) as described below.

All CsMPs were of an almost spherical or distorted spherical shape, and their diameter distribution ranged from 1.2 to 3.0  $\mu\text{m}$  with the same mean and median values of 1.8  $\mu\text{m}$ . The  $^{137}\text{Cs}$  radioactivity of the single CsMP varied from 0.13 to 0.87 Bq/granule, and the mean and median values of  $^{137}\text{Cs}$  radioactivity were 0.35 Bq/granule and 0.36 Bq/granule, respectively. The  $^{134}\text{Cs}$  radioactivity was less than the detection limit in most cases due to its shorter physical half-life of about 2 years than that of  $^{137}\text{Cs}$ . The elemental mapping images (a) and EDS spectra (b) of #11-HNVF-300601-Q are given in Fig. 3. It is obvious that Cs in the particle showed multiple peaks (Cs

$\text{L}\alpha$  and Cs  $\text{L}\beta$  at 4.42 and 4.55 keV), and O, Si, Na, S, Cl, K, Ca, Ti, Fe, and Zn also coexisted within the particle according to the elemental mapping images of major elements. Moreover, based on EDS analysis of 15 CsMPs, the main elemental components included Si (average atomic mass fraction  $36.0 \pm 5.3$  wt.%), O ( $50.1 \pm 3.7$  wt.%), Cs ( $1.0 \pm 0.2$  wt.%), Zn ( $2.7 \pm 1.0$  wt.%), Sn ( $0.2 \pm 0.2$  wt.%), S ( $0.1 \pm 0.1$  wt.%), Na ( $3.2 \pm 3.3$  wt.%), K ( $2.5 \pm 2.2$  wt.%), Fe ( $1.0 \pm 0.3$  wt.%), Cl ( $0.2 \pm 0.1$  wt.%), and some other trace elements in some individual particles, such as Ba, Al, P, Ca, and Ti. The elemental composition of each CsMPs is given in Additional file 1: Table S1.

The water insolubility of radiocesium in CsMPs has been reported by Adachi et al. (Adachi et al. 2013), and other reports also support this fact [CsMPs can be isolated from the wet-isolation method (Imoto et al. 2017; Kurihara et al. 2020a) and can be detected in river water (Miura et al. 2018)]. The water insolubility of the CsMPs was also checked by immersion of the isolated A-CsMPs into water for 24 h (#11-NHVF-300601-Q) and 48 h (#12-NHVF-300906-Q), which is shown in Additional file 1: Fig. S1. There was no obvious detectable change in their radiocesium activity and seeable change in morphology before and after the immersion. Therefore, we conclude that CsMPs exhibit very low water-solubility in short term. Regarding the long-term solubility, there have been a few research (Miura et al. 2018; Okumura et al. 2019). The morphology, the  $^{137}\text{Cs}$  radioactivity, the elemental compositions and distributions, and the water insolubility of isolated CsMPs in this study were consistent with those of the reported type A CsMPs (Adachi et al. 2013; Igarashi et al. 2019a; Satou et al. 2018; Abe et al. 2014). We can conclude that type A CsMPs are detected in aerosol samples and refer to aerosol CsMPs as “A-CsMPs.”

#### 3.1.2 Comparison of CsMPs isolated from aerosols and soil

There are 24 CsMPs detected in soil sample (namely, ten granules per gram, which was approximately consistent with the results of Ikehara et al. (2020)) and we refer to these soil CsMPs as “S-CsMPs.” The  $^{137}\text{Cs}$  radioactivity of these S-CsMPs mostly ranged from 0.06 to 0.95 Bq/granule, except for one that exhibited 6.70 Bq. Their mean and median values were 0.29 and 0.22 Bq/granule, respectively, and the sum of  $^{137}\text{Cs}$  radioactivity of these S-CsMPs was 13.4 Bq. Six single granules from the group of 24 S-CsMPs have thus far been successfully extracted from the soil samples, and three of them have been observed and analyzed by SEM–EDS. The SEM images and their elemental compositions are given in Fig. 4 and Additional file 1: Table S2, respectively. They were all spherical particles, and their diameters were 1.8  $\mu\text{m}$  (S-CsMPs-1, 0.93 Bq/granule), 1.6  $\mu\text{m}$  (S-CsMPs-2,

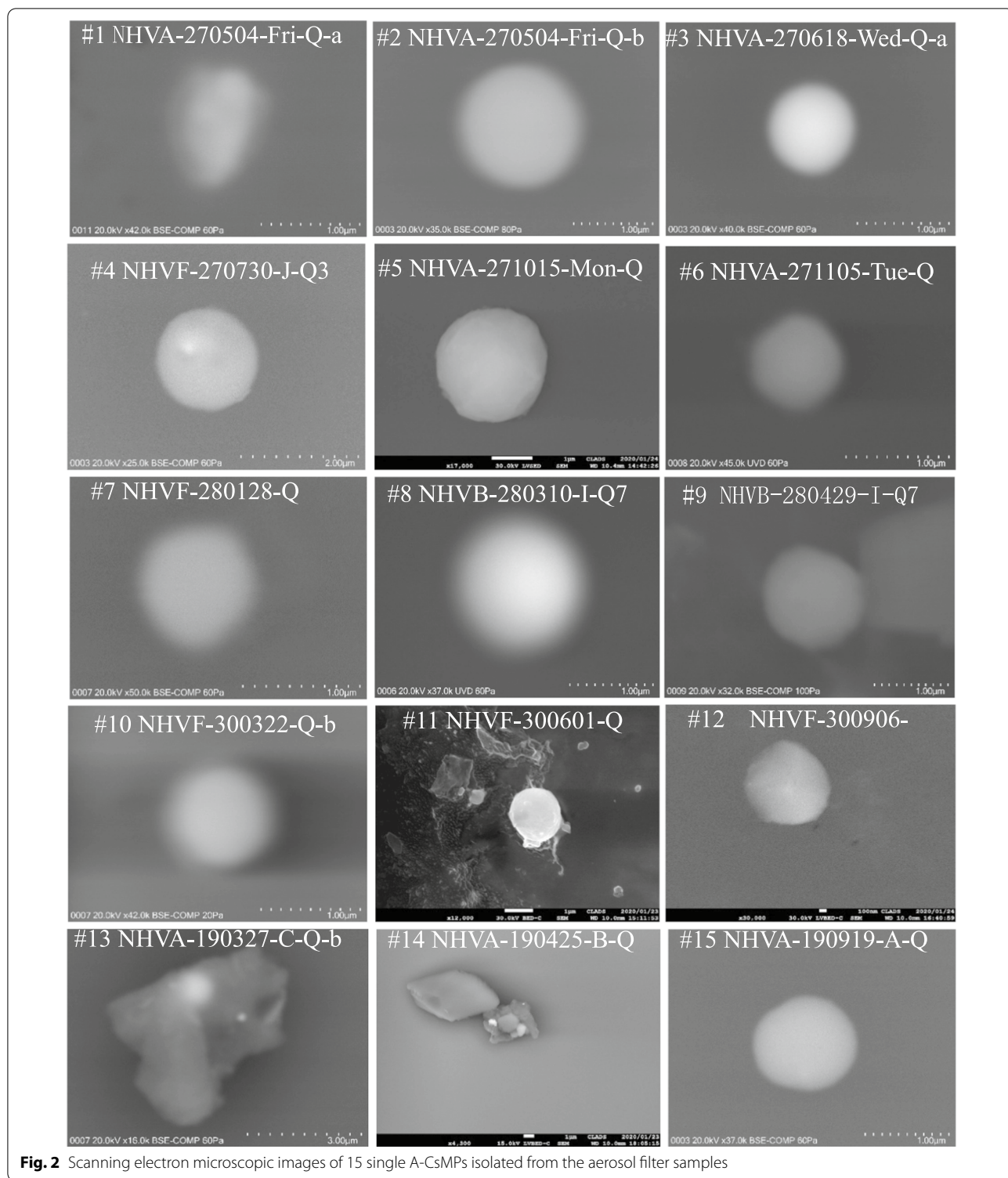


**Fig. 2** Scanning electron microscopic images of 15 single A-CsMPs isolated from the aerosol filter samples

0.56 Bq/granule), and 1.8  $\mu\text{m}$  (S-CsMPs-3, 0.75 Bq/granule), with an average diameter of  $1.7 \pm 0.1 \mu\text{m}$  ( $0.75 \pm 0.18$  Bq/granule).

Moreover, the EDS spectra of an A-CsMP (#15-HNVA-190919) and an S-CsMP (S-CsMPs-3) are shown in comparison in Fig. 5. These EDS spectra showed that both A-CsMPs and S-CsMPs mainly consist of Si, O, Cs, Fe,

**Table 1** Information of 15 single isolated insoluble Cs-bearing particles (The radioactivity is corrected back to 11/03/2011 14:46, JST)

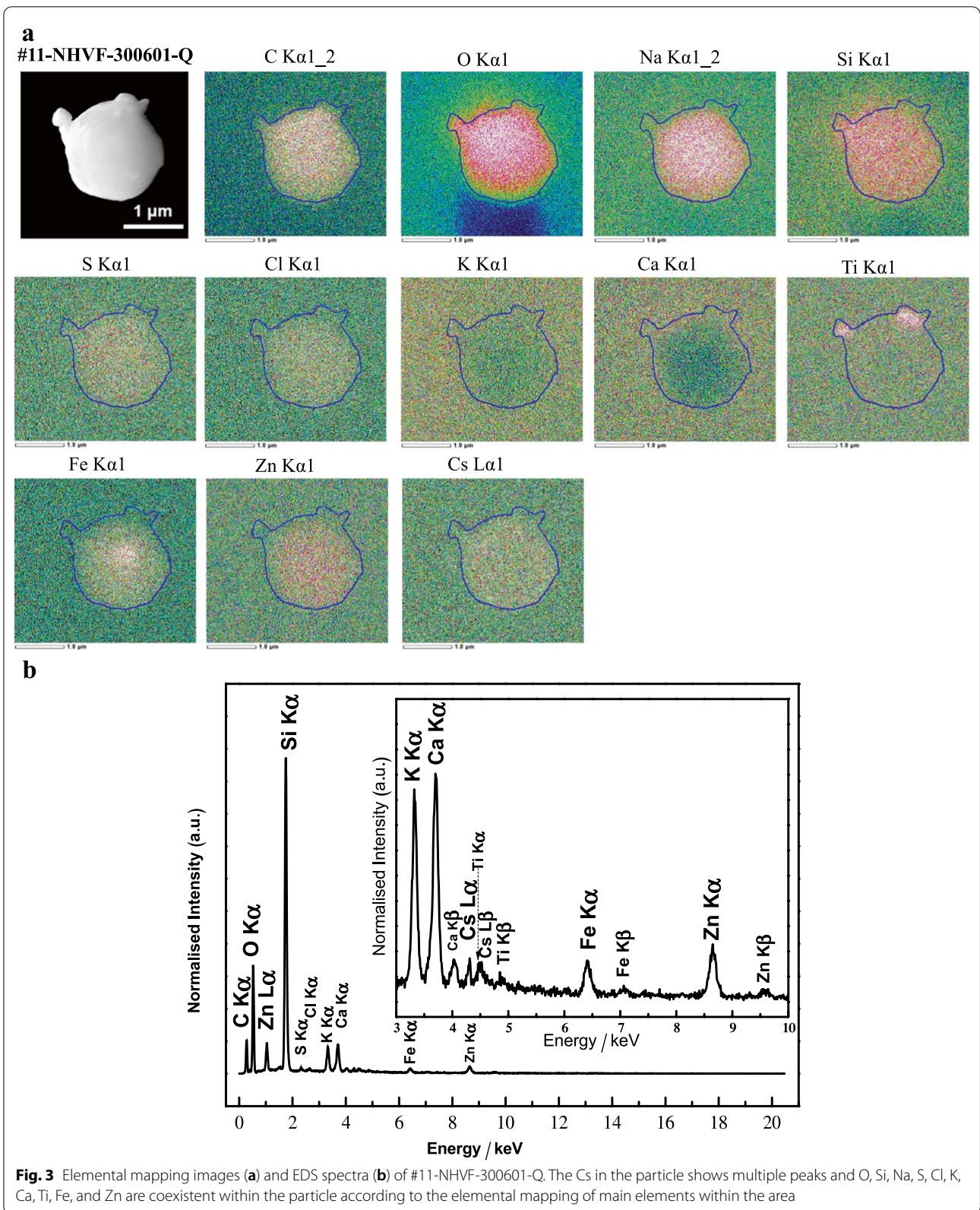
| No.    | Sample name         | <sup>137</sup> Cs (Bq) in filter (T) | <sup>137</sup> Cs (Bq) per granule (P) | Resuspension contribution ratio of CsMPs ( $\frac{P}{T} \times 100\%$ ) | D / $\mu\text{m}$ |
|--------|---------------------|--------------------------------------|--|---|-------------------|
| 1      | NHVA-270504_Fri-Q-a | 2.03                                 | 0.18                                   | 8.7%  | 1.2               |
| 2      | NHVA-270504_Fri-Q-b | 2.03                                 | 0.40                                   | 20.1%   | 2.0               |
| 3      | NHVA-270618_Wed-Q-a | 1.53                                 | 0.13                                   | 8.6%  | 1.7               |
| 4      | NHVF-270730-J-Q3    | 2.44                                 | 0.38                                   | 15.7%   | 1.2               |
| 5      | NHVA-271015_Mon-Q   | 1.77                                 | 0.36                                   | 20.5%   | 2.5               |
| 6      | NHVA-271105_Tue-Q   | 1.61                                 | 0.13                                   | 8.3%  | 1.9               |
| 7      | NHVF-280128-Q       | 0.84                                 | 0.17                                   | 20.6%   | 1.8               |
| 8      | NHVB-280310-I-Q7    | 1.36                                 | 0.67                                   | 49.5%   | 1.4               |
| 9      | NHVB-280429-I-Q7    | 1.91                                 | 0.52                                   | 27.0%   | 1.8               |
| 10     | NHVF-300322-Q-b     | 1.16                                 | 0.17                                   | 15.0%   | 1.5               |
| 11     | NHVF-300601-Q       | 1.73                                 | 0.87                                   | 50.6%   | 2.0               |
| 12     | NHVF-300906-Q       | 3.55                                 | 0.18                                   | 5.0%  | 1.4               |
| 13     | NHVA-190327-C-Q-b   | 0.65                                 | 0.17                                   | 25.6%   | 3.0               |
| 14     | NHVA-190425-B-Q     | 1.36                                 | 0.60                                   | 43.9%   | 2.0               |
| 15     | NHVA-190919-A-Q     | 0.90                                 | 0.36                                   | 39.2%   | 1.2               |
| Mean   | 1.66                | 0.35                                 | 23.9%                                  | 1.8   |                   |
| Median | 1.61                | 0.36                                 | 20.5%                                  | 1.8   |                   |

Zn, K, Na, and Cl. Specifically, the average atomic mass fraction of the main elemental compositions of the three S-CsMPs were evaluated, given as following; Si ( $6.4 \pm 6.7$  wt.%), O ( $29.2 \pm 4.7$  wt.%), Cs ( $1.7 \pm 2.48$  wt.%), Zn ( $3.5 \pm 4.6$  wt.%), Fe ( $1.9 \pm 2.4$ ), Na ( $1.0 \pm 0.7$  wt.%), K ( $0.3 \pm 0.4$  wt.%) and Cl ( $0.4 \pm 0.6$  wt.%). The radiocesium activities, morphologies, and elemental compositions of A-CsMPs and S-CsMPs were almost consistent with each other. These results imply that A-CsMPs were derived from the resuspension of S-CsMPs.

### 3.2 Possibility of natural resuspension of CsMPs into the atmosphere

The possibility of CsMP resuspension from the contaminated surface soil was suggested in studies (Ishizuka et al. 2017; Higaki et al. 2020; Nihei et al. 2018; Utsunomiya et al. 2019). Specifically, CsMPs were detected in face masks worn by Fukushima residents in the spring of 2013 (Higaki et al. 2020). The resuspended CsMPs were also found on Japanese mustard spinach in Fukushima Prefecture cultivated from August to December 2017 (Nihei et al. 2018). The resuspension of radiocesium caused by decontamination work has also been reported by several studies (Ikehara et al. 2020; Hosoda et al. 2019; Doi et al. 2018), suggesting a possibility of the resuspension of the CsMPs induced by decontamination work by the government. However, these studies have not discussed whether the resuspension of CsMPs into the atmosphere can occur naturally or not because CsMPs in these studies

were found in living areas or in association with human activities. In contrast, A-CsMPs of this study were found in aerosol samples collected by unmanned-operated HV samplers at a site located in an evacuated area that was difficult for residents to return to, indicating the possibility that A-CsMPs were derived from naturally resuspended S-CsMPs, without anthropogenic activities. Furthermore, it is possible that the A-CsMPs were transported from F1NPP or areas where decontamination and other remediation activities were carried out. If a significant number of radioactive pollutants, including CsMPs, were transported to the sampling site, the atmospheric concentration of <sup>137</sup>Cs should have increased. However, a systematic increase in atmospheric <sup>137</sup>Cs concentration was not detected during the sampling periods of A-CsMPs, and no leakage events of radioactive pollutants from the F1NPP were reported. These results imply a low likelihood that A-CsMPs were derived from decontamination work at the F1NPP site and the severely contaminated areas. On the one hand, transport of contaminated soil by dump trucks has increased along a road near the sampling site since 2018, and decontamination activities in areas adjacent to the sampling sites (within 500 m range) were also conducted between June and December 2019. On the other hand, there was no increasing trend in the detected numbers of A-CsMPs in 2015, 2016, 2018, and 2019. More specifically, only one A-CsMP was found after June 2019, as shown in Table 2. Therefore, it seems unlikely that A-CsMPs in this study were derived from human activities.





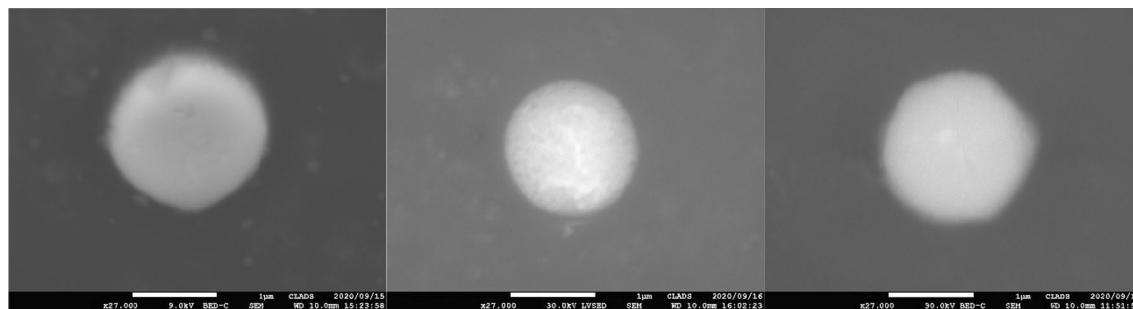


**Fig. 4** Scanning electron microscopic images of 3 single S-CsMPs isolated from the soil samples (The average diameter of all spherical S-CsMPs was  $1.7 \pm 0.1 \mu\text{m}$ , which is conspicuously close to that of A-CsMPs)

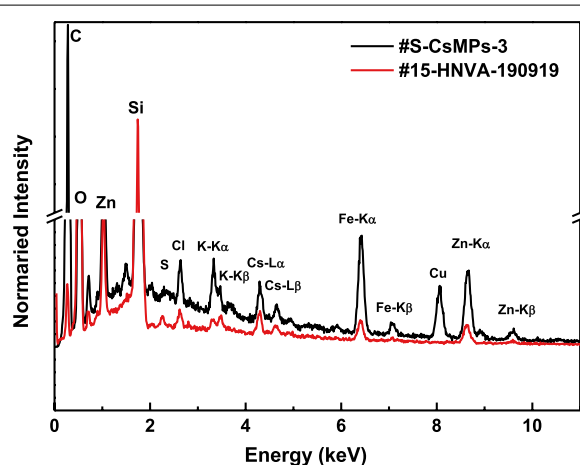


**Fig. 5** Energy-dispersive X-ray spectrum of A-CsMPs (#15-HNVA-190919) and S-CsMPs-3. (Cu and C are derived from copper and carbon tape substrates, which were used to confirm the existence of silicon and the fixation of CsMPs)

Significantly, we can find that the atomic ratios of Na/Si ( $\approx 0.086$ ), K/Si ( $\approx 0.045$ ), and/or Cs/Si ( $\approx 0.031$ ) of our isolated A-CsMPs are smaller than that of the CsMPs ( $\sim 0.139$  /  $\sim 0.055$  /  $\sim 0.040$ ) released in the early stage (approximately 6 months after the Fukushima accident) (Okumura et al. 2020), even lower than that of the CsMPs collected at far distance away from F1NNP (Cs/Si  $\approx 0.208$ ) (Utsunomiya et al. 2019), herein, the concentration of Cs has been corrected back to March 11, 2011, 14:46 JST, and assuming that there has been no decrease in Si. This special characteristic of our isolated A-CsMPs quantitatively exemplifies the high possibility of A-CsMPs resulted from the resuspension of S-CsMPs. This phenomenon may be attributed to the slow environmental erosion by the loss of the very small amount of Na and K, even the loss of Cs, which is consistent with the report of slow environmental weathering dissolvable CsMPs (Okumura et al. 2019). This information of

lowering the Cs concentration with time lapse implies mitigation of the anxieties for the hazard resulting from the resuspension of the CsMPs. Moreover, we observed a typical suspension phenomenon of surface soil on April 22, 2021, in the playground of Ibaraki University, where have similarly environmental circumstances as our sampling site. It can indirectly provide the natural resuspension condition of CsMPs by the wind gust of which speed exceeding  $4 \text{ m s}^{-1}$ , as shown in Additional file 1: Fig. S2 and Additional file 2: Supporting video.

### 3.3 Resuspension frequencies of CsMPs

In this study, 165 aerosol filter samples collected over 4 years (2015, 2016, 2018, and 2019) were used to detect and isolate the CsMPs. Although they were not all aerosol samples because of time and cost considerations, the sampling periods of the used samples (165 samples) covered more than 80% of the total sampling period:  $290.5(\text{days})/365(\text{days})$  in 2015,  $352.5/366$  in 2016,  $346.5/365$  in 2018, and  $225.5/274$  in 2019, and  $1215/1461 = 0.83$  overall. As mentioned above, 20 highly radioactive granules were detected in these 165 samples, and 15 single A-CsMPs have been successfully obtained. The detailed data for A-CsMPs and aerosol filters are given in Tables 1, 2, and Additional file 1: Table S3. If all 20 CsMPs were A-CsMPs, the sampling probability of A-CsMPs at the sampling site can be estimated as  $1.6 \times 10^{-2}$  granule per sampling day or  $1.2 \times 10^{-5}$  granule per unit sampling-air volume ( $\text{m}^{-3}$ ).

Furthermore, the yearly frequency was obtained as follows:  $2.1 \times 10^{-2}$  granule $\cdot\text{day}^{-1}$  in 2015,  $8.5 \times 10^{-3}$  granule $\cdot\text{day}^{-1}$  in 2016,  $8.7 \times 10^{-3}$  granule $\cdot\text{day}^{-1}$  in 2018, and  $1.3 \times 10^{-2}$  granule $\cdot\text{day}^{-1}$  in 2019. There was no considerable decreasing trend of these resuspension frequencies, which strongly suggests necessity of the long-term monitoring of resuspended CsMPs. Alternatively, the seasonal frequency variation of resuspended A-CsMPs can be found in Table 2. The number

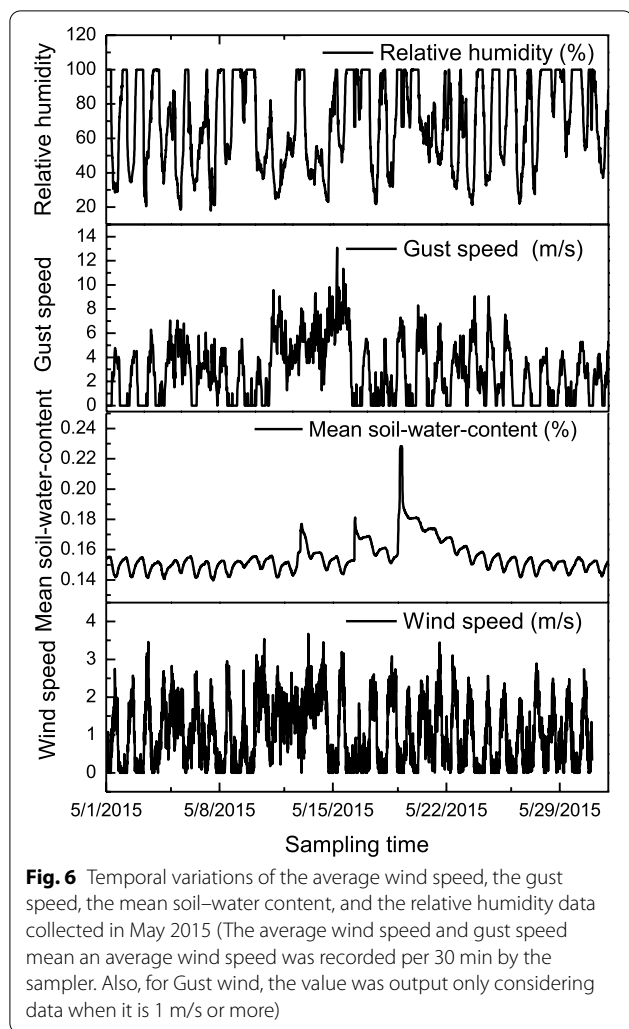
**Table 2** Seasonal or yearly frequency variations of 15 single isolated insoluble CsMPs

| Sampling year             |                      | Jan   | Feb | Mar  | Apr  | May | Jun | Jul | Aug | Sep  | Oct | Nov | Dec  | Total  | Yearly frequency                               |
|---------------------------|----------------------|-------|-----|------|------|-----|-----|-----|-----|------|-----|-----|------|--|--|
| 2015                      | Number of CsMPs      | 0     | 0   | 0    | 0    | 2   | 1   | 1   | 0   | 0    | 2   | 0   | 0    | 6  | $2.1 \times 10^{-2}$ granule-day <sup>-1</sup> |
|                           | Sampling period/days | 18    | 0   | 14   | 14.5 | 31  | 30  | 31  | 31  | 30   | 31  | 29  | 31   | 290.5  |  |
| 2016                      | Number of CsMPs      | 1     | 0   | 1    | 1    | 0   | 0   | 0   | 0   | 0    | 0   | 0   | 0    | 3  | $8.5 \times 10^{-3}$ granule-day <sup>-1</sup> |
|                           | Sampling period/days | 31    | 29  | 31   | 30   | 31  | 30  | 31  | 31  | 30   | 31  | 30  | 17.5 | 352.5  |  |
| 2018                      | Number of CsMPs      | 0     | 0   | 1    | 0    | 1   | 0   | 0   | 1   | 0    | 0   | 0   | 0    | 3  | $8.7 \times 10^{-3}$ granule-day <sup>-1</sup> |
|                           | Sampling period/days | 12.5  | 28  | 31   | 30   | 31  | 30  | 31  | 31  | 30   | 31  | 30  | 31   | 346.5  |  |
| 2019                      | Number of CsMPs      | 0     | 0   | 1    | 1    | 0   | 0   | 0   | 1   | 0    | 0   | 0   | 0    | 3  | $1.3 \times 10^{-2}$ granule-day <sup>-1</sup> |
|                           | Sampling period/days | 23.5  | 0   | 30.5 | 30   | 31  | 30  | 31  | 31  | 18.5 | 0   | 0   | 0    | 225.5  |  |
| <b>Seasonal frequency</b> |                      |       |     |      |      |     |     |     |     |      |     |     |      |  |  |
| Dec.–Feb. (DJF)           | Number of CsMPs      | 1     |     |      |      |     |     |     |     |      |     |     |      | $4.5 \times 10^{-3}$ granule-day <sup>-1</sup> |  |
|                           | Sampling period/days | 221.5 |     |      |      |     |     |     |     |      |     |     |      |  |  |
| Mar.–May (MAM)            | Number of CsMPs      | 8     |     |      |      |     |     |     |     |      |     |     |      | $2.4 \times 10^{-2}$ granule-day <sup>-1</sup> |  |
|                           | Sampling period/days | 335   |     |      |      |     |     |     |     |      |     |     |      |  |  |
| Jun.–Aug. (JJA)           | Number of CsMPs      | 4     |     |      |      |     |     |     |     |      |     |     |      | $1.1 \times 10^{-2}$ granule-day <sup>-1</sup> |  |
|                           | Sampling period/days | 368   |     |      |      |     |     |     |     |      |     |     |      |  |  |
| Sep.–Nov. (SON)           | Number of CsMPs      | 2     |     |      |      |     |     |     |     |      |     |     |      | $6.9 \times 10^{-3}$ granule-day <sup>-1</sup> |  |
|                           | Sampling period/days | 290.5 |     |      |      |     |     |     |     |      |     |     |      |  |  |

and seasonal frequencies of A-CsMPs detected in four seasons of four sampling years are as follows: (a) 1 and  $4.5 \times 10^{-3}$  granule-day<sup>-1</sup> in December–February (DJF), (b) 8 and  $2.4 \times 10^{-2}$  granule-day<sup>-1</sup> in March–May (MAM), (c) 4 and  $1.1 \times 10^{-2}$  granule-day<sup>-1</sup> in Jun–August, and (d) 2 and  $6.9 \times 10^{-3}$  granule-day<sup>-1</sup> in September–November. The seasonal frequency tended lower in DJF and higher in MAM. In DJF the surface soil is mostly frozen or very wet, and snow often covers the ground at the sampling site (Ishizuka et al. 2017), and these conditions can inhibit the resuspension of CsMPs from the surface soil in this season. Kinase et al. (2018) showed that soil mineral particles were major coarse aerosols at our sampling site in the springtime (MAM), indicating that the suspension of soil particles from the ground surface occurred in this season. It is reasonable and possible that this dispersion process may cause the resuspension of CsMPs. Kinase et al. (2018) also found that the peak of the atmospheric radiocesium concentration was consistent with maximal average wind speed in the springtime. Based on the above discussion, it would be obvious that the atmospheric radiocesium concentration was associated with wind-driven suspended soil in the springtime. This seasonality is consistent with the natural resuspension of the CsMPs in this study.

Meteorological data, including the gust, the average wind speeds (the wind speeds were sampled at a height of approximately 10 m from the ground), the mean soil–water content, and the relative humidity (RH), were measured at the sampling site in 2015, when six CsMPs

were sampled. These data from May 2015 are plotted in Fig. 6. Two CsMPs were collected when the wind gust speed exceeded  $4 \text{ m s}^{-1}$  and the soil water content was not notably high (significantly, during the sampling time, wind gust speeds exceeding  $4 \text{ m s}^{-1}$  can be frequently observed and sometimes even exceeded  $8 \text{ m s}^{-1}$ , as shown in Fig. 6 and Additional file 1: Fig. S3). Furthermore, Wu et al. (1992) observed that particles (with diameters ranging from 7.0 to 42.3  $\mu\text{m}$ ) could be suspended occasionally at wind speeds of  $4 \text{ m s}^{-1}$ , with more than half of the particles suspended within 2 s at a wind speed of  $8 \text{ m s}^{-1}$ . Nicholson (1993) obtained a gentle increasing trend for suspension of particles with a 4.1  $\mu\text{m}$  diameter along with increments of wind speed, and a positive correlation between  $\text{PM}_{2.5}$  and a wind speed higher than  $3 \text{ m s}^{-1}$  was also found by Wang and Ogawa (2015). These characteristics of microparticle suspension can indirectly explain the resuspension of CsMPs and the low frequency of A-CsMP detection in this work. Additionally, Ishizuka et al. (2017) developed a size-resolved suspension scheme for soil particles from the ground surface to estimate and explain measured size distribution of resuspended radioactive particles at the sampling site same as ours. They found that the particle size distributions of radioactive particles, adopting sandy loam and silty loam as soil textures, were in good agreement with that of the particles with diameters ranging around 1–2  $\mu\text{m}$  in the size-resolved atmospheric radioactivity concentration observation. Thus, natural resuspension of CsMPs with diameter of 1–2  $\mu\text{m}$  by wind could be



possibly and reasonably observed when wind speed was high and soil moisture was low. Especially, the large scale of a SEM image of a representative aerosol filter sample collected on May 16, 2016, as shown in Additional file 1: Fig. S4, exhibits many microparticles from topsoil, which can also be observed in the report of Kaneyasu et al. (Kaneyasu et al. 2017). Obviously, it was almost impossible to find the location of a CsMP in a filter or soil sample before isolation. However, these observations confirmed the resuspension of CsMPs absorbing/attaching on surface soil by strong winds. Also, in Fig. 2, it can be found that the isolated aerosol CsMPs (#9 NHVB-280429-I-Q7 and #14 NHVA-190425-B-Q) were still adsorbed on other large particles. In addition, in our isolated S-CsMPs, the phenomenon of S-CsMPs absorbing other particles was not clear, but it was able to find in the reports of Satou et al. (2018) (samples of FT-13#01 and NM-14#02). These results further supported the resuspension mechanism of CsMPs: they are readily absorbed/

attached on topsoil particles and resuspended into air by high wind speed. Therefore, we speculate that CsMP resuspension needs both a strong wind of  $4 \text{ m s}^{-1}$  and incidental phenomena such as aggregate lumps formed by attachment/collisions of CsMPs with larger dust particles scattered by winds. Furthermore, according to SEM observations of aerosol CsMPs and soil CsMPs, the possibility of soil dust working as the carriers of the resuspended CsMPs is high. Moreover, it is unable to exclude CsMP resuspended by itself, obtained from the reasons: (1) the high CsMPs concentration of 10 granules/gram in the surface soil of our sampling site, (2) high resuspension frequency of CsMPs in spring when major suspended particles sampled there was soil dust, and (3) the reports of Ishizuka et al. (2017) that the particle size distributions of radioactive particles, adopting sandy loam and silty loam as soil textures, were in good agreement with that of the particles with diameters ranging around  $1\text{--}2 \mu\text{m}$  in the size-resolved atmospheric radioactivity concentration observation. However, the organic matter works as the carrier of the resuspended CsMPs were not clear in this study. Additionally, because some holes that were presumably dug by wild boars were found around the sampling site (within a few hundred meters), a possibility, that the dispersion of CsMPs occurred with such animal activities, cannot be ruled out. It is a great challenge to discuss more detailed information by random appearance of wild animals in the sampling location, also, this consideration is waiting for more observations.

### 3.4 Contribution of the resuspended CsMPs to atmospheric radioactivity

Various studies (Ikehara et al. 2020, 2018) have shown that significant levels of CsMPs were released into the environment (Furuki et al. 2017) and that a considerable part of the deposition of radiocesium should be attributed to the released CsMPs (Imoto et al. 2017; Utsunomiya et al. 2019). Based on the results and discussion above, CsMPs can be directly resuspended into atmosphere. Herein, the contribution ratio of the resuspended CsMPs to atmospheric  $^{137}\text{Cs}$  can be defined as the ratio of the radioactivity of single CsMPs ( $^{137}\text{Cs}$ ) to that of the aerosol filters from which the A-CsMPs was obtained. As given in Table 2, the resuspension contribution ratios of CsMPs ranged from 5.0 to 50.6%, and the mean and median values were 23.9% and 20.5%, respectively. The remainder of the resuspension hosts of atmospheric radiocesium can be attributed to bioaerosols and soil particles bearing with low concentrations of radiocesium (Igarashi et al. 2019b; Kita et al. 2020) as well as low-level radioactive CsMPs. Although A-CsMPs were not detected by one-hour exposure by IP, the radioactive spot was detected in the aerosol filter by IP inspection

when the IP plate was exposed for tens of hours, as shown in Additional file 1: Fig. S5. Because of the excessive amount of time and human resources required for the extraction procedure, further extraction of CsMPs in these filters has not been conducted. Moreover, the average contribution ratio of A-CsMPs, which is the ratio of total  $^{137}\text{Cs}$  radioactivity of 15 A-CsMPs to that of all 165 aerosol samples, was estimated to be about 2.0%, as shown in Additional file 1: Table S3. Correspondingly, the ratio of total  $^{137}\text{Cs}$  radioactivity of S-CsMPs to that of the surface soil sample used in this study was about 8.0% (= 13.40 Bq/166.2 Bq); the contribution of A-CsMPs to the total atmospheric radioactivity, therefore, was smaller than that in the corresponding surface soil.

#### 4 Conclusions

This study reveals the occurrence of direct resuspension of water-insoluble CsMPs, composed of silicate glass, to the atmosphere without human interference. The fact can be confirmed by (1) their successful extraction from aerosol samples collected by unmanned-operated samplers, (2) the nearly resembling characteristics of A-CsMPs and S-CsMPs, which were extracted from the respective aerosol and surface soil samples collected at the same sampling site in a heavily contaminated area of F1NPP and (3) the seasonality of the A-CsMP detection. The sizes and radioactivities of both A-CsMPs and S-CsMPs found in the present study were situated within the distributions of the reported type A CsMPs, but they were generally smaller than those reported for type A CsMPs (with a diameter of less than ca. 10  $\mu\text{m}$ ) (Adachi et al. 2013; Abe et al. 2014) sampled in primary emission from the F1NPP accident in 2011. This can be used to exclude the probability that A-CsMPs may be derived from the primary release and may be explained by surface-deposited CsMPs subjected to their very slow dissolution rates in the natural environment, as suggested by Okumura et al. (Okumura et al. 2019). Therefore, the erosion of CsMPs in the natural environment should be a significant process to be clarified by future studies.

This study also reveals the frequency of CsMP resuspension and its contribution to atmospheric radiocesium, although this can vary with the location depending on the amount of radiocesium and CsMP deposition (surface contamination extent). The resuspension of insoluble type A CsMPs is indeed infrequent, and their absolute activity remains at the sub-Bq level. On the other hand, the detection of type A CsMPs has been continued up to 2019 and no obvious decreasing trend has been found from annual resuspension frequencies, suggesting its persistence. The CsMPs can also work as the transferring medium of fuel debris (Ochiai et al. 2018), trace uranium (Abe et al. 2014; Kurihara et al. 2020a), strontium (Zhang

et al. 2019), and plutonium (Kurihara et al. 2020b) into the environment, although they are at very low level, and CsMPs resuspension increases the possibility of unpredictable inhalation. If they are inhaled, they can easily reach the deep respiratory system (Assessment N. C. f. E., NC 1996). Thus, more investigation is necessary regarding the risk assessment of even the single CsMP radiation exposure (Suzuki et al. 2020) and long-term monitoring of these resuspended insoluble type A CsMPs.

#### Abbreviations

F1NPP: Fukushima Daiichi Nuclear Power Plant; CsMPs: Radiocesium-bearing microparticles; A-CsMPs: Aerosol radiocesium-bearing microparticles; S-CsMPs: Soil radiocesium-bearing microparticles; JAEA: Japan Atomic Energy Agency; MRI: Meteorological Research Institute; TEPCO: Tokyo Electric Power Company.

#### Supplementary Information

The online version contains supplementary material available at <https://doi.org/10.1186/s40645-022-00475-6>.

**Additional file 1.** Supporting figures and tables.

**Additional file 2.** Supporting video: suspension of surface soil.

#### Acknowledgements

We thank Ms. N. Hayashi, Mr. K. Minami, Ms. H. Li, and other students of the College of Science and College of Engineering, Ibaraki University, for the maintenance of the sampling instruments, special installations in the field, and data collection. We especially thank the local government of Namie and the Fukushima prefectural government, who kindly provided the monitoring opportunity. We also acknowledge Mr. K. Hama (Atox Co. Ltd) and Mr. K. Obara for assistance with the activity measurements and separation of A-CsMPs.

#### Authors' contributions

PT and KH analyzed the samples and summarized these data in this article. PT prepared the manuscript. KK planned and carried out the measurements as well as the samplings. YI is the leader of our project team. KK and YI helped in writing the manuscript and provided important discussions for this article. YS, KA, and TK supported the measurement of the aerosol and soil CsMPs by SEM-EDS. KN and AS collected and measured radioactivity of the soil samples. YS and KA also provided important suggestions for this article. All authors read and approved the final manuscript.

#### Authors' information

PT received his Ph.D. from University of Fukui in 2020 and worked at Ibaraki University as a postdoctoral researcher and wrote this article during this period.

KK received his Ph.D. from Tokyo University in 1990 and worked at Tokyo University until 2002 as a research assistant. He moved to Ibaraki University in 2002. His studies focus on the atmospheric  $\text{O}_3$  and  $\text{NO}_2$ , the effects of black carbon (BC) on global warming, and the resuspension processes of radiocesium.

YI received his Ph.D. from the University of Tsukuba in 1987. From 1987 to 1991, he worked at the former National Institute of Radiological Sciences and moved to the MRI in 1991. His current interests are atmospheric aerosols; their precursors, including Asian dust and  $\text{PM}_{2.5}$ ; their possible influences on climate and general environmental changes and other related phenomena.

YS received his Ph.D. from University of Tsukuba in 2016, worked as researcher in Collaborative Laboratories for Advanced Decommissioning Sciences, Japan Atomic Energy Agency. His current interests are focused on the research of F1NPP accident released radioactive particles.

KA received his Ph.D. from Kobe University in 2005, worked at Arizona State University between 2005 and 2011 as a postdoctoral/faculty research associate, and is currently studying atmospheric aerosols at the MRI.

TK received his Ph.D. from Ibaraki University in 2016. His interests are focusing on BC aerosols and Environmental Transfer of Radionuclides from the Fukushima Daiichi NPP Accident.

KN received his Ph.D. from Osaka University in 2007 and worked at Osaka University in 2008. He moved to JAEA and worked as a research scientist between 2009 and 2012; then, he returned to Osaka University. His main research field is nuclear- and radiochemistry.

AS received his Ph.D. from Osaka University in 1985 and then worked at the Japan Society for the Promotion of Science. He moved to Nagoya University, where he worked between 1987 and 1998. Then, he moved to Kyoto University in 1998, before moving to Osaka University in 1999. His main research field is nuclear and radiochemistry.

#### Funding

This study was financially supported by Nuclear Energy Science & Technology and Human Resource Development Project (International Joint Research Program of Nuclear Decommission of Japan-UK, 30I125) and partly by Grants-in-Aid for Scientific Research (B) (Nos. 20H04318 and 17H01873).

#### Availability of data and materials

The datasets supporting the conclusions of this study are available as additional files (Supporting information file and Supporting video of suspension of surface soil) and are available upon request to the corresponding authors, Kazuyuki Kita (E-mail: kazuyuki.kita.iu@vc.ibaraki.ac.jp) and Yasuhito Igarashi (E-mail: igarashi.yasuhito.4e@kyoto-u.ac.jp).

#### Declarations

#### Competing interests

The authors declare that they have no competing interests.

#### Author details

<sup>1</sup>Graduate School of Science and Engineering, Ibaraki University, 2-1-1 Bunkyo, Mito, Ibaraki 310-8512, Japan. <sup>2</sup>Institute for Integrated Radiation and Nuclear Science, Kyoto University, 2-chome, Asashiro-Nishi, Kumatori, Sennan, Osaka 590-0494, Japan. <sup>3</sup>Collaborative Laboratories for Advanced Decommissioning Science (CLADS), Japan Atomic Energy Agency (JAEA), 790-1 Otsuka, Motoooka, Tomioka, Fukushima 979-1195, Japan. <sup>4</sup>Meteorological Research Institute (MRI), Japan Meteorological Agency (JMA), 1-1 Nagamine, Tsukuba, Ibaraki 305-0052, Japan. <sup>5</sup>Japan Agency for Marine-Science and Technology, Research Institute for Global Change (RIGC), Institute of Arctic Climate and Environment Research (IACE), 3173-25 Showa-machi, Kanazawa, Yokohama, Kanagawa 236-0001, Japan. <sup>6</sup>Graduate School of Science, Osaka University, 1-1 Machikaneyama, Toyonaka, Osaka 560-0043, Japan.

Received: 20 August 2021 Accepted: 28 February 2022

Published online: 14 March 2022

#### References

- Abe Y, Iizawa Y, Terada Y, Adachi K, Igarashi Y, Nakai I (2014) Detection of uranium and chemical state analysis of individual radioactive microparticles emitted from the Fukushima nuclear accident using multiple synchrotron radiation X-ray analyses. *Anal Chem* 86(17):8521–8525
- Adachi K, Kajino M, Zaizen Y, Igarashi Y (2013) Emission of spherical cesium-bearing particles from an early stage of the Fukushima nuclear accident. *Sci Rep* 3(1):2554
- Akimoto K (2015) Annual and weekly cycles of radioactivity concentration observed in Fukushima city. *Health Phys* 108(1):32–38
- Aoyama M, Tsumune D, Inomata Y, Tateda Y (2020) Mass balance and latest fluxes of radiocesium derived from the Fukushima accident in the western North Pacific Ocean and coastal regions of Japan. *J Environ Radioact* 217:106206
- Assessment (1996) N. C. f. E.; (NC) Air quality criteria for particulate matter. US Environmental Protection Agency, Office of Research and Development, vol 3
- Doi T, Takagi M, Tanaka A, Kanno M, Dokiya Y, Tao Y, Masumoto K (2018) The variation of atmospheric radioactive caesium concentration from Fukushima Dai-ichi Nuclear Power Plant Accident in Tsukuba and Iitate, and factors controlling its high concentration events. *Radioisotopes* 68(3):83–104 (in Japanese)
- EPA (1977) Proposed guidance on dose limits for persons exposed to transuranium elements in the general environment. US Environmental Protection Agency
- Evrard O, Lacey JP, Nakao A (2019) Effectiveness of landscape decontamination following the Fukushima nuclear accident: a review. *SOIL* 5(2):333–350
- Fuchigami M, Kasahara N (2015) 2 - The Fukushima nuclear power plant accident: the main sequence of events. Yotaro H, Seiji A, Masao F, Naoto K (eds) *The 2011 Fukushima Nuclear Power Plant Accident*, Woodhead Publishing, 2015: pp 21–96. <https://doi.org/10.1016/B978-0-08-100118-9.00002-4>.
- Furuki G, Imoto J, Ochiai A, Yamasaki S, Nanba K, Ohnuki T, Grambow B, Ewing RC, Utsunomiya S (2017) Caesium-rich micro-particles: A window into the meltdown events at the Fukushima Daiichi Nuclear Power Plant. *Sci Rep* 7(1):42731
- Garger E, Gordeev S, Hollaender W, Kashparov V, Kashpur V, Martinez-Serrano J, Mironov V, Peres J, Tschiersch J, Vintersved I, Watterson J (1996) Resuspension and deposition of radionuclides under various conditions. Belarus: N. p. [https://inis.iaea.org/collection/NCLCollectionStore/\\_Public/31/056/31056833.pdf](https://inis.iaea.org/collection/NCLCollectionStore/_Public/31/056/31056833.pdf)
- Garger E, Talerko M (2020) Re-entrainment of the Chernobyl-derived radionuclides in air: experimental data and modeling. *Behav Radionucl Environ* 11:75
- Hatamura Y, Abe S, Fuchigami M, Kasahara N, Iino K (2014) The 2011 Fukushima nuclear power plant accident: how and why it happened, vol 73. Woodhead Publishing, Sawston
- Hidaka A (2019) Formation mechanisms of insoluble Cs particles observed in Kanto district four days after Fukushima Daiichi NPP accident. *J Nucl Sci Technol* 56(9–10):831–841
- Higaki S, Shirai H, Hirota M, Takeda E, Yano Y, Shibata A, Mishima Y, Yamamoto H, Miyazawa K (2014) Quantitation of Japanese cedar pollen and radiocesium adhered to nonwoven fabric masks worn by the general population. *Health Phys* 107(2):117–134
- Higaki S, Kurihara Y, Takahashi Y (2020) Discovery of radiocesium-bearing particles in masks worn by members of the public in Fukushima in spring 2013. *Health Phys* 118(6):656–663
- Hirose K (2013) Temporal variation of monthly <sup>137</sup>Cs deposition observed in Japan: effects of the Fukushima Daiichi nuclear power plant accident. *Appl Radiat and Isotop* 81:325–329
- Hirose K (2016) Fukushima Daiichi Nuclear Plant accident: atmospheric and oceanic impacts over the five years. *J Environ Radioact* 157:113–130
- Hirose K (2020) Atmospheric effects of Fukushima nuclear accident: a review from a sight of atmospheric monitoring. *J Environ Radioact* 218:106240
- Hosoda M, Hozumi W, Akata N, Endo A, Kelleher K, Yamanouchi K, Imajo Y, Fukuhara T, Shiroma Y, Iwaoka K, Tokonami S (2019) Evaluations of inventory and concentration of radiocesium in soil at a residential house 3 years after Fukushima nuclear accident. *Radiat Prot Dosim* 184(3–4):518–522
- Igarashi Y, Kajino M, Zaizen Y, Adachi K, Mikami M (2015) Atmospheric radioactivity over Tsukuba, Japan: a summary of three years of observations after the FDNPP accident. *Prog Earth Planet Sci* 2(1):44
- Igarashi Y, Kogure T, Kurihara Y, Miura H, Okumura T, Satou Y, Takahashi Y, Yamaguchi N (2019a) A review of Cs-bearing microparticles in the environment emitted by the Fukushima Dai-ichi Nuclear Power Plant accident. *J Environ Radioact* 205–206:101–118
- Igarashi Y, Kita K, Maki T, Kinase T, Hayashi N, Hosaka K, Adachi K, Kajino M, Ishizuka M, Sekiyama TT, Zaizen Y, Takenaka C, Ninomiya K, Okochi H, Sorimachi A (2019b) Fungal spore involvement in the resuspension of radiocaesium in summer. *Sci Rep* 9(1):1954
- Ikehara R, Suetake M, Komiya T, Furuki G, Ochiai A, Yamasaki S, Bower WR, Law GTW, Ohnuki T, Grambow B, Ewing RC, Utsunomiya S (2018) Novel method of quantifying radioactive cesium-rich microparticles (CSMPs) in the environment from the Fukushima Daiichi Nuclear Power Plant. *Environ Sci Technol* 52(11):6390–6398
- Ikehara R, Morooka K, Suetake M, Komiya T, Kurihara E, Takehara M, Takami R, Kino C, Horie K, Takehara M (2020) Abundance and distribution of radioactive cesium-rich microparticles released from the Fukushima Daiichi Nuclear Power Plant into the environment. *Chemosphere* 241:125019

- Imoto J, Ochiai A, Furuki G, Suetake M, Ikehara R, Horie K, Takehara M, Yamasaki S, Nanba K, Ohnuki T, Law GTW, Grambow B, Ewing RC, Utsunomiya S (2017) Isotopic signature and nano-texture of cesium-rich micro-particles: Release of uranium and fission products from the Fukushima Daiichi Nuclear Power Plant. *Sci Rep* 7(1):5409
- Investigation Committee on the Accident at the Fukushima Nuclear Power Station of Tokyo Electric Power Company (2011) Cabinet Secretariat of the Government of Japan, Tokyo, Japan, Interim Report
- Ishizuka M, Mikami M, Tanaka TY, Igarashi Y, Kita K, Yamada Y, Yoshida N, Toyoda S, Satou Y, Kinase T, Ninomiya K, Shinohara A (2017) Use of a size-resolved 1-D resuspension scheme to evaluate resuspended radioactive material associated with mineral dust particles from the ground surface. *J Environ Radioact* 166:436–448
- Kajino M, Ishizuka M, Igarashi Y, Kita K, Yoshikawa C, Inatsu M (2016) Long-term assessment of airborne radiocesium after the Fukushima nuclear accident: re-suspension from bare soil and forest ecosystems. *Atmos Chem Phys* 16:13149–13172
- Kaneyasu N, Ohashi H, Suzuki F, Okuda T, Ikemori F (2012) Sulfate aerosol as a potential transport medium of radiocesium from the Fukushima nuclear accident. *Environ Sci Technol* 46(11):5720–5726
- Kaneyasu N, Ohashi H, Suzuki F, Okuda T, Ikemori F, Akata N, Kogure T (2017) Weak size dependence of resuspended radiocesium adsorbed on soil particles collected after the Fukushima nuclear accident. *J Environ Radioact* 172:122–129
- Kinase T, Kita K, Igarashi Y, Adachi K, Ninomiya K, Shinohara A, Okochi H, Ogata H, Ishizuka M, Toyoda S, Yamada K, Yoshida N, Zaizen Y, Mikami M, Demizu H, Onda Y (2018) The seasonal variations of atmospheric  $^{134}\text{Cs}$  and  $^{137}\text{Cs}$  activity and possible host particles for their resuspension in the contaminated areas of Tsushima and Yamakiya, Fukushima, Japan. *Prog Earth Planet Sci* 5(1):12
- Kita K, Igarashi Y, Kinase T, Hayashi N, Ishizuka M, Adachi K, Koitabashi M, Sekiyama TT, Onda Y (2020) Rain-induced bioecological resuspension of radiocesium in a polluted forest in Japan. *Sci Rep* 10(1):1–15
- Kita K, Hayashi N, Minami K, Kimura M, Igarashi Y, Adachi K, Maki T, Ishizuka M, Okochi H, Furukawa J, Ninomiya K, Shinohara A (2018) Increase of radioactive cesium resuspension to the atmosphere with bioaerosols in a polluted area in Fukushima. *EGUGA*, 7773
- Kurihara Y, Takahata N, Yokoyama TD, Miura H, Kon Y, Takagi T, Higaki S, Yamaguchi N, Sano Y, Takahashi Y (2020a) Isotopic ratios of uranium and caesium in spherical radioactive caesium-bearing microparticles derived from the Fukushima Dai-ichi Nuclear Power Plant. *Sci Rep* 10(1):3281
- Kurihara E, Takehara M, Suetake M, Ikehara R, Komiya T, Morooka K, Takami R, Yamasaki S, Ohnuki T, Horie K, Takehara M, Law GTW, Bower WW, Mosselmanns JF, Warnicke P, Grambow B, Ewing RC, Utsunomiya S (2020b) Particulate plutonium released from the Fukushima Daiichi meltdown. *Sci Total Environ* 743:140539
- Matsuda N, Mikami S, Shimoura S, Takahashi J, Nakano M, Shimada K, Uno K, Hagiwara S, Saito K (2015) Depth profiles of radioactive cesium in soil using a scraper plate over a wide area surrounding the Fukushima Dai-ichi Nuclear Power Plant, Japan. *J Environ Radioact* 139:427–434
- Mishra S, Aree H, Sorimachi A, Hosoda M, Tokonami S, Ishikawa T, Sahoo SK (2015) Distribution and retention of Cs radioisotopes in soil affected by Fukushima nuclear plant accident. *J Soils Sedim* 15(2):374–380
- Miura H, Kurihara Y, Sakaguchi A, Tanaka K, Yamaguchi N, Higaki S, Takahashi Y (2018) Discovery of radiocesium-bearing microparticles in river water and their influence on the solid-water distribution coefficient (Kd) of radiocesium in the Kuchibuto River in Fukushima. *Geochem J* 52(2):145–154
- Miura H, Ishimaru T, Ito Y, Kurihara Y, Otosaka S, Sakaguchi A, Misumi K, Tsunune D, Kubo A, Higaki S (2021) First isolation and analysis of caesium-bearing microparticles from marine samples in the pacific coastal area near Fukushima Prefecture. *Sci Rep* 11(1):1–11
- Nakagawa M, Yamada K, Toyoda S, Kita K, Igarashi Y, Komatsu S, Yamada K, Yoshida N (2018) Characterization of hydrocarbons in aerosols and investigation of biogenic sources as a carrier of radiocesium isotopes. *Geochem J* 52(2):163–172
- Nakamura AJ (2020) Assessment of DNA damage induction in farm animals after the FNPP accident. Low-dose radiation effects on animals and ecosystems. Springer, Singapore, pp 153–161
- Nicholson K (1993) Wind tunnel experiments on the resuspension of particulate material. *Atmos Environ A Gen Top* 27(2):181–188
- Nihei N, Yoshimura K, Okumura T, Tanoi K, Iijima K, Kogure T, Nakanishi TM (2018) Secondary radiocesium contamination of agricultural products by resuspended matter. *J Radioanal Nucl Chem* 318(1):341–346
- Niimura N, Kikuchi K, Tuyen ND, Komatsuzaki M, Motohashi Y (2015) Physical properties, structure, and shape of radioactive Cs from the Fukushima Daiichi Nuclear Power Plant accident derived from soil, bamboo and shiitake mushroom measurements. *J Environ Radioact* 139:234–239
- Ochiai S, Hasegawa H, Kakiuchi H, Akata N, Ueda S, Tokonami S, Hisamatsu S (2016) Temporal variation of post-accident atmospheric  $^{137}\text{Cs}$  in an evacuated area of Fukushima Prefecture: size-dependent behaviors of  $^{137}\text{Cs}$ -bearing particles. *J Environ Radioact* 165:131–139
- Ochiai A, Imoto J, Suetake M, Komiya T, Furuki G, Ikehara R, Yamasaki S, Law GTW, Ohnuki T, Grambow B, Ewing RC, Utsunomiya S (2018) Uranium dioxides and debris fragments released to the environment with cesium-rich microparticles from the Fukushima Daiichi Nuclear Power Plant. *Environ Sci Technol* 52(5):2586–2594
- Okumura T, Yamaguchi N, Dohi T, Iijima K, Kogure T (2019) Dissolution behaviour of radiocesium-bearing microparticles released from the Fukushima nuclear plant. *Sci Rep* 9(1):3520
- Okumura T, Yamaguchi N, Suga H, Takahashi Y, Segawa H, Kogure T (2020) Reactor environment during the Fukushima nuclear accident inferred from radiocesium-bearing microparticles. *Sci Rep* 10(1):1–9
- Onda Y, Kato H, Hoshi M, Takahashi Y, Nguyen M-L (2015) Soil sampling and analytical strategies for mapping fallout in nuclear emergencies based on the Fukushima Dai-ichi Nuclear Power Plant accident. *J Environ Radioact* 139:300–307
- Press C (2015) CRC handbook of chemistry and physics-table of isotopes
- Satou Y, Sueki K, Sasa K, Adachi K, Igarashi Y (2016) First successful isolation of radioactive particles from soil near the Fukushima Daiichi Nuclear Power Plant. *Anthropocene* 14:71–76
- Satou Y, Sueki K, Sasa K, Yoshikawa H, Nakama S, Minowa H, Abe Y, Nakai I, Ono T, Adachi K, Igarashi Y (2018) Analysis of two forms of radioactive particles emitted during the early stages of the Fukushima Dai-ichi Nuclear Power Station accident. *Geochem J* 52(2):137–143
- Shannon S (2012) Radiation protective foods: a menu for the nuclear age
- Snow MS, Snyder DC, Delmore JE (2016) Fukushima Daiichi reactor source term attribution using cesium isotope ratios from contaminated environmental samples. *Rapid Commun Mass Spectrom* 30(4):523–532
- Steinhauser G, Brandl A, Johnson TE (2014) Comparison of the Chernobyl and Fukushima nuclear accidents: a review of the environmental impacts. *Sci Total Environ* 470–471:800–817
- Suzuki M, Ninomiya K, Satou Y, Sueki K, Fukumoto M (2020) Perspective on the biological impact of exposure to radioactive cesium-bearing insoluble particles. Low-dose radiation effects on animals and ecosystems. Springer, Singapore, pp 205–213
- Tanaka K, Takahashi Y, Sakaguchi A, Umeko M, Hayakawa S, Tanida H, Saito T, Kanai Y (2012) Vertical profiles of iodine-131 and cesium-137 in soils in Fukushima prefecture related to the Fukushima Daiichi Nuclear Power Station accident. *Geochem J* 46(1):73–76
- Tokyo Electric Power Company Holdings (2011) I. T. Fukushima nuclear accident analysis report (interim report) summary
- Utsunomiya S, Furuki G, Ochiai A, Yamasaki S, Nanba K, Grambow B, Ewing RC (2019) Caesium fallout in Tokyo on 15th March, 2011 is dominated by highly radioactive, caesium-rich microparticles. <http://arxiv.org/abs/1906.00212>.
- Wagenpfeil F, Tschiersch J (2001) Resuspension of coarse fuel hot particles in the Chernobyl area. *J Environ Radioact* 52(1):5–16
- Wang J, Ogawa S (2015) Effects of meteorological conditions on PM<sub>2.5</sub> concentrations in Nagasaki, Japan. *Int J Environ Res Public Health* 12(8):9089–9101
- Wu Y-L, Davidson CI, Russell AG (1992) Controlled wind tunnel experiments for particle bounceoff and resuspension. *Aerosol Sci Technol* 17(4):245–262
- Yamaguchi N, Eguchi S, Fujiwara H, Hayashi K, Tsukada H (2012) Radiocesium and radioiodine in soil particles agitated by agricultural practices: field observation after the Fukushima nuclear accident. *Sci Total Environ* 425:128–134
- Yamamoto K, Nomura S, Tsubokura M, Murakami M, Ozaki A, Leppold C, Sawano T, Takita M, Kato S, Kanazawa Y, Anbe H (2019) Internal exposure risk due to radiocesium and the consuming behaviour of local foodstuffs among pregnant women in Minamisoma City near the Fukushima

nuclear power plant: a retrospective observational study. *BMJ Open* 9(7):e023654

- Yoschenko VI, Kashparov VA, Protsak VP, Lundin SM, Levchuk SE, Kadygrib AM, Zvarich SI, Khomutinin YV, Maloshtan IM, Lanshin VP, Kovtun MV, Tschiersch J (2006) Resuspension and redistribution of radionuclides during grassland and forest fires in the Chernobyl exclusion zone: part I. Fire experiments. *J Environ Radioact* 86(2):143–163
- Yoshida N, Kanda J (2012) Tracking the Fukushima radionuclides. *Science* 336(6085):1115
- Yoshida N, Takahashi Y (2012) Land-surface contamination by radionuclides from the Fukushima Daiichi Nuclear Power Plant accident. *Elements* 8(3):201–206
- Zhang Z, Igarashi J, Satou Y, Ninomiya K, Sueki K, Shinohara A (2019) Activity of  $^{90}\text{Sr}$  in fallout particles collected in the difficult-to-return zone around the Fukushima Daiichi Nuclear Power Plant. *Environ Sci Technol* 53(10):5868–5876

### Publisher's Note

Springer Nature remains neutral with regard to jurisdictional claims in published maps and institutional affiliations.

Submit your manuscript to a SpringerOpen<sup>®</sup> journal and benefit from:

- ▶ Convenient online submission
- ▶ Rigorous peer review
- ▶ Open access: articles freely available online
- ▶ High visibility within the field
- ▶ Retaining the copyright to your article

---

Submit your next manuscript at ▶ [springeropen.com](https://www.springeropen.com)

---